Chinese Chemical Letters 35 (2024) 108574

Contents lists available at ScienceDirect

Chinese Chemical Letters

journal homepage: www.elsevier.com/locate/cclet

A nonenzymatic electrochemical sensor for the detection of hydrogen peroxide *in vitro* and *in vivo* fibrosis models

Hongyao Liu[a,1], Yan Yu[b,1], Taixiong Xue[a], Cailing Gan[a], Yuting Xie[a], Doudou Wang[a], Peilin Li[a], Zhiyong Qian[b,*], Tinghong Ye[a,*]

[a] Department of Gastroenterology and Hepatology, Sichuan University-University of Oxford Huaxi Joint Centre for Gastrointestinal Cancer and Frontiers Science Center for Disease-Related Molecular Network, State Key Laboratory of Biotherapy, West China Hospital, Sichuan University, Chengdu 610041, China
[b] Department of Biotherapy, Cancer Center and State Key Laboratory of Biotherapy, West China Hospital, Sichuan University, Chengdu 610041, China

ARTICLE INFO

Article history:
Received 21 March 2023
Revised 11 May 2023
Accepted 14 May 2023
Available online 20 May 2023

Keywords:
Fibrosis
H_2O_2
Electrochemical sensor
NOX4
Nintedanib

ABSTRACT

Fibrosis occurs due to the excessive deposition of extracellular matrix caused by cell injury. After various types of tissue injury, the dysregulation of the internal response can eventually lead to the destruction of organ structure and dysfunction. There is increasing evidence that oxidative stress, which is characterized by excessive production of hydrogen peroxide (H_2O_2), is an important cause of fibrosis. Therefore, we synthesized a biosensitive and efficient electrochemical H_2O_2 sensor based on PtNi nanoparticle-doped N-reduced graphene oxide (PtNi-N-rGO) to detect H_2O_2 released from transforming growth factor β1 (TGFβ1)-induced myofibroblast. In addition, the sensor could easily detect changes in H_2O_2 in the lung and bronchoalveolar lavage fluid (BALF) of mice with pulmonary fibrosis. Furthermore, the sensor could also detect H_2O_2 in activated hepatic stellate cells and the liver of carbon tetrachloride (CCl_4)-induced liver fibrosis. Moreover, the alterations in H_2O_2 detected by the sensor were consistent with nicotinamide adenine dinucleotide phosphate oxidase 4 (NOX4) protein expression and the staining results of pathological sections. Taken together, these results highlight the use of H_2O_2 sensors for the rapid detection of fibrosis and facilitate the rapid evaluation of antifibrotic drug candidates.

Fibrosis is considered to be an abnormal repair process in connective tissue caused by various chronic injuries, such as massive levels of apoptosis or necrosis. Nearly half of the deaths from various diseases are associated with organ tissue fibrosis, which is a common feature of chronic diseases that affects nearly every tissue in the body [1,2]. Studies of idiopathic pulmonary fibrosis (IPF) have shown that fibrosis enhances the deposition of extracellular matrix (ECM) proteins produced by myofibroblasts. The pathogenesis of this disease is unclear, and the prognosis is poor, with a 5-year survival rate that is worse than that of many common cancers [3–5]. More importantly, with the global spread of corona virus disease 2019 (COVID-19), some severe and critically ill patients may develop pulmonary fibrosis due to inflammation and injury, which has increased public health awareness [6]. High-resolution computed tomography (HRCT) is the main diagnostic method for IPF [7]. During liver fibrosis, hepatic stellate cells (HSCs) in the resting state are stimulated by various inflammatory factors, such as transforming growth factor β1 (TGFβ1) to form myofibroblasts, which secrete ECM and participate in the development of liver fibrosis [8]. There are striking similarities in profibrotic signalling cascades during fibrosis, and TGFβ1 is associated with the stimulation of ECM production, reactive oxygen species (ROS) production, and the fibroblast to myofibroblast transition, which are the main events in tissue fibrosis [9–11]. Excess ROS and reactive free radicals are produced in the liver, which weakens the antioxidant function of the liver, leads to an increase in reactive free radicals in liver cells and impairs the normal function of cells, eventually leading to necrosis and apoptosis in hepatocytes [12]. Although studies have shown that this process is reversible, there is currently no clinically approved drug to treat this condition, and inhibiting oxidative stress is an important means of treating liver injury and liver fibrosis. Furthermore, evaluating whether drugs can inhibit cell oxidative stress, maintain cell membrane stability, and detect tissue oxidation indices are the main methods of evaluating antifibrotic drugs [13–15].

Compared with other organs, the lungs are particularly susceptible to oxidative stress, and after external stimuli such as radiation, drugs, and the environment induce lung damage, inflammatory factors such as TGFβ1 stimulate excessive ECM deposition,

* Corresponding authors.
E-mail addresses: anderson-qian@163.com (Z. Qian), yeth1309@scu.edu.cn (T. Ye).
[1] These authors contributed equally to this work.

https://doi.org/10.1016/j.cclet.2023.108574
1001-8417/

and lung fibroblasts are activated and further promote ROS production, which is the main manifestation of pulmonary fibrosis [16,17]. Since oxidative stress leads to pathological wound healing and fibrosis, previous research has shown that inhibitors of ROS generation generally have antifibrotic effects [18]. NOX4 is a complex enzyme whose structure leads to the formation of H_2O_2, which plays an important role in TGFβ-mediated signal transduction [19]. Elevated NOX4 levels have also been reported in IPF lungs [20]. In ageing mice, NOX4 expression is elevated, and the ability of these animals to resolve fibrosis is reduced [21]. Fibrosis can be regulated by regulating H_2O_2 levels in cells. Further studies have confirmed that the NOX4 inhibitor GKT137831 decreases H_2O_2 levels, reduces intracellular oxidative stress and enables reparative cell transplantation to restore lung and liver regeneration [22]. NOX4 knockdown during hepatic fibrosis not only inhibits ROS production but also reduces the expression of alpha-smooth muscle actin (α-SMA) in angiotensin II-induced LX2 cells [23]. Therefore, we hypothesize that the upregulation of H_2O_2 may be used as a biomarker for the diagnosis of fibrosis.

Detecting H_2O_2 in tissues is a challenge due to the low levels of H_2O_2 in tissues, its short half-life, and its instability. In addition, other detection methods, such as fluorescence and chemiluminescence techniques, either have low sensitivity or complex sample preparation, making it difficult to achieve real-time and rapid measurement of H_2O_2 [24]. However, with the rapid development of materials science, biology, electrochemistry and other disciplines, great progress has been made in electrochemical sensing technology [25,26]. In our previous study, we detected H_2O_2 in cancer cells using nonenzymatic hydrogen peroxide electrochemical sensing, which was also used to efficiently detect tumour tissue, adjacent tissue, and normal tissue. Due to the complex mechanism and unknown aetiology of fibrosis and the complicated and lengthy drug screening process [28,29], it is necessary to establish a more accurate and convenient fibrosis diagnosis method.

Here, we successfully detected H_2O_2 released by TGFβ1-induced fibroblasts using a nonenzymatic chemical sensor, which also conveniently detected changes in H_2O_2 in the lung and BALF of mice with pulmonary fibrosis. In addition, the sensor could detect H_2O_2 in activated hepatic stellate cells and the liver of mice with hepatic fibrosis. The changes in H_2O_2 detected by the sensor were consistent with NOX4 protein expression and the staining results of pathological sections. Taken together, these results highlight the use of H_2O_2 sensors for the rapid detection of fibrosis disease progression and facilitate the rapid evaluation of antifibrotic drug candidates.

Our previous findings have confirmed that this H_2O_2 sensor has good sensor performance, including safety, selectivity, repeatability and stability [27]. Therefore, we first characterize the structure of composite nanomaterials by measuring the size, distribution and morphology of nanoparticles. The size and morphology of the PtNi-N-rGO nanocomposites were characterized by transmission electron microscopy (TEM). Typical TEM images are shown in Figs. 1a and b and adequately demonstrate that the PtNi nanoparticles were evenly distributed and easily supported on folded rGO nanosheets. The lattice fringes of the PtNi nanoparticles are shown in Fig. 1c. High-resolution transmission electron microscopy (HRTEM) images show interplanar distances of 0.21 nm and 0.18 nm (Fig. 1c). The average size of the nanoparticles was approximately 5 nm (Fig. 1d). Energy dispersive spectroscopy (EDS) further confirmed the presence of C, O, N, Pt and Ni atoms in the nanocomposites (Fig. 1e). The distributions of Pt and Ni were further demonstrated by EDS line-scan profiles of individual nanoparticles (Fig. 1f). These data indicate that the PtNi-N-rGO nanocomposites were successfully synthesized.

It is well established that TGFβ1 induces fibroblast activation and epithelial-mesenchymal transformation (EMT), and so we first

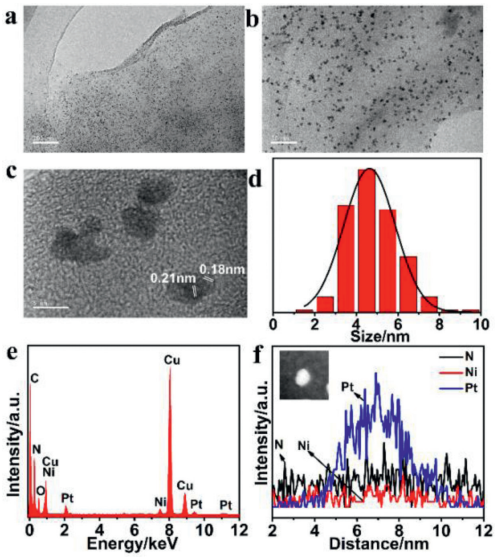

Fig. 1. (a, b) TEM images of PtNi-N-rGO. Scale bars: 200 nm (a) and 50 nm (b); (c) HRTEM image of PtNi-N-rGO. Scale bar: 5 nm; (d) the size distribution of PtNi nanoparticles; (e) EDS spectrum of PtNi-N-rGO; (f) scanning transmission electron microscopy (STEM) image and EDS line profiles of a single PtNi-N-rGO nanoparticle.

examined changes in intracellular ROS levels after TGFβ1 stimulation. As shown in Fig. S1 (Supporting information), the NIH-3T3, A549 and LX2 cell lines released more ROS after TGFβ1 stimulation while the ROS level decreased after the nintedanib intervention. Next, we investigated whether the as-fabricated H_2O_2 sensor could be used to detect H_2O_2 released by activated fibroblasts using commercially available H_2O_2 kits for comparison. Figs. 2a–d shows that the H_2O_2 sensor had an obvious response to H_2O_2 released by NIH-3T3 and A549 cells after TGFβ1 stimulation. More importantly, a reduction in H_2O_2 levels was detected after the cells were treated with nintedanib. These results were confirmed by commercially available H_2O_2 test kits (Figs. S2a and b in Supporting information). During TGFβ1-induced fibrosis, epithelial cells gradually lose their characteristics and gain the characteristics of mesenchymal cells [28]. As shown in Figs. 2e and f, in response to TGFβ1 stimulation, the protein expression of collagen I in NIH-3T3 cells was increased, and the protein expression of E-cadherin in A549 cells was decreased. The expression of NOX4 is consistent in these two types of cells. However, nintedanib reversed these changes in protein expression in activated cells. In addition, TGFβ1 changed the morphology of A549 cells compared to control, including hypertrophy, elongation, and spindle shape. These results suggest that H_2O_2 levels are positively correlated with TGFβ1-induced fibrosis progression in NIH-3T3 and A549 cell models.

It is important to highlight the fact that the commercially available kit generates trivalent iron ions by oxidizing divalent iron ions with H_2O_2, and then forms a purple product with xylenol orange in a specific solution to determine the concentration of H_2O_2. The natural microenvironmental characteristics of sensors and cells could have a profound impact on the reactivity and sensitivity of sensors. In contrast, no apparent current response was observed when catalase was injected prior to the addition of *N*-formylmethionyl-leucyl-phenyl-alanine (fMLP) (Fig. S3 in Supporting information). This finding suggests that the response current was due to fMLP-induced H_2O_2 release from activated fibroblasts. Therefore, this may be one of the reasons for the increased sensitivity of electrochemical sensors for H_2O_2.

A pulmonary fibrosis model was established by a single intratracheal instillation of bleomycin (BLM) to mice (approximately 2 mg/kg) [28,30]. Animal experimental procedure was permitted

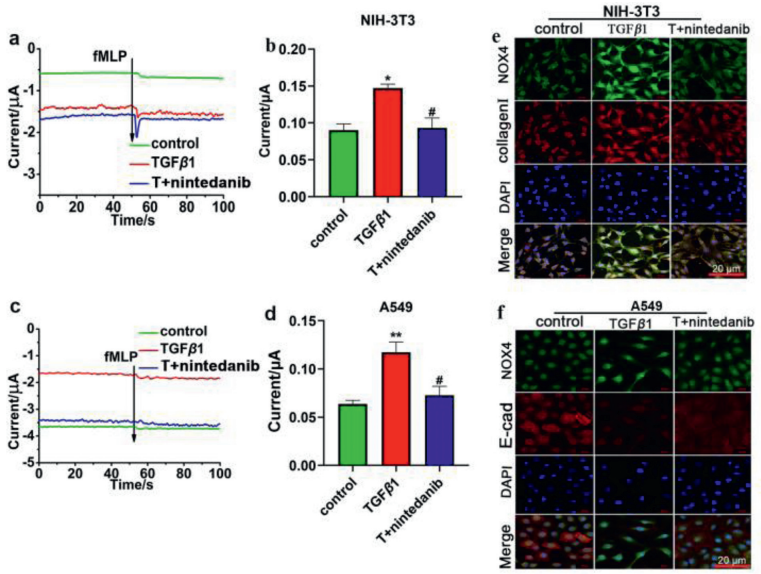

Fig. 2. (a–d) Statistical results of the current response in cells detected by the sensor. The values are expressed as the mean ± standard deviation (SD), $n = 3$. $^{*}P < 0.05$, $^{**}P < 0.01$ compared with control; $^{\#}P < 0.05$ compared with TGFβ1. (e, f) NOX4 immunofluorescence imaging of NIH-3T3 cells and A549 cells with collagen I or E-cadherin. Scale bar: 20 μm. DAPI, diamidino-phenyl-indole.

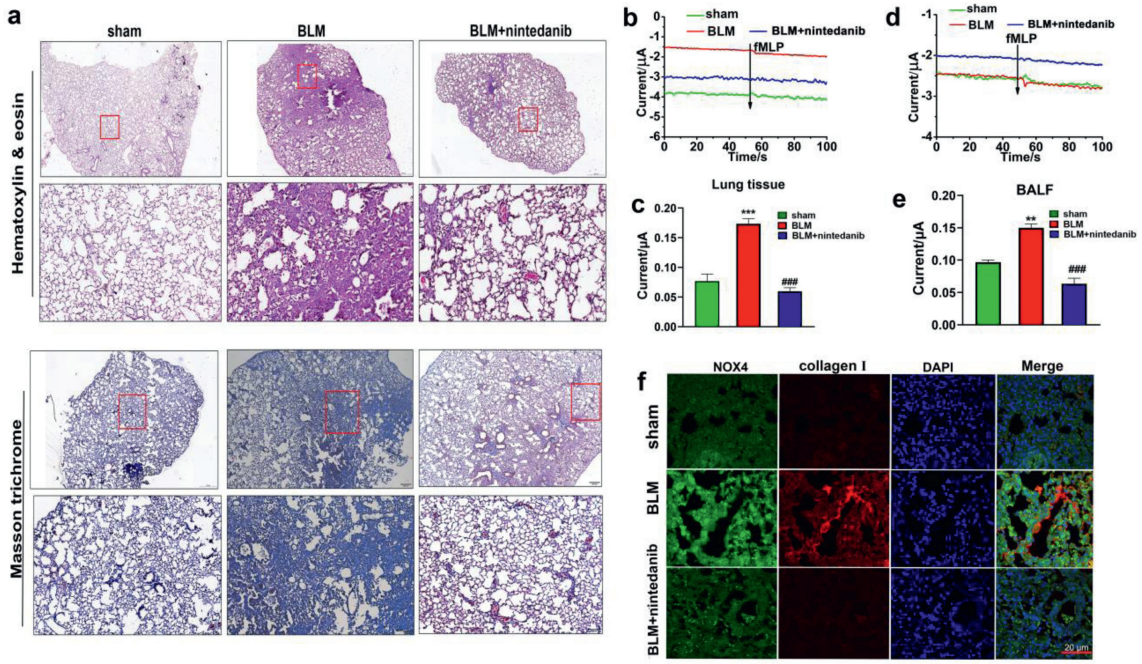

Fig. 3. (a) H&E staining and Masson staining of lung tissue. Scale bar: 200 and 100 μm. (b, c) The levels of H_2O_2 in the lung of mice were detected by the sensor. (d, e) The levels of H_2O_2 in the BALF of mice were detected by the sensor. The data are presented as the means ± SD, $n = 3$. $^{**}P < 0.01$, $^{***}P < 0.001$ *vs.* sham. $^{\#\#\#}P < 0.001$ *vs.* BLM. (f) Immunofluorescence imaging of collagen I and NOX4 in lung tissues. Scale bar: 20 μm.

the Institutional Animal Care and Treatment Committee of Sichuan University in China (New Permit Number: 20220531039). As illustrated in Fig. 3a, the success of BLM-induced pulmonary fibrosis was confirmed by hematoxylin and eosin (H&E) and Masson's trichrome staining, which are classic histochemical methods to detect inflammation and fibrosis [31]. H_2O_2 levels in lung tissue lysate (Figs. 3b and c) and BALF (Figs. 3d and e) after BLM treatment was significantly increased compared with those in the sham group, while nintedanib treatment group was significantly decreased. More importantly, NOX4 protein expression was consistent with the *in vitro* results. Immunofluorescence analysis showed that NOX4 protein levels near areas of collagen deposition were up-regulated and enriched in fibrotic lesions after BLM treatment (Fig. 3f). In conclusion, H_2O_2 levels in fibrotic lungs increased with increasing pulmonary fibrosis levels. In addition, we detected oxidative stress in the lung of mice with fibrosis. Compared with those in the sham group, after BLM exposure, oxidative stress indices in the lung, including the levels of malondialdehyde (MDA), superoxide dismutase (SOD) and H_2O_2, were significantly increased (Figs. S2d–f in Supporting information), indicating that BLM induced severe oxidative stress in lung tissues.

To explore whether our electrochemical sensor could detect H_2O_2 in fibrotic liver, we constructed animal models of hepatic fibrosis [29] (Fig. 4e), and nintedanib was used to validate the sen-

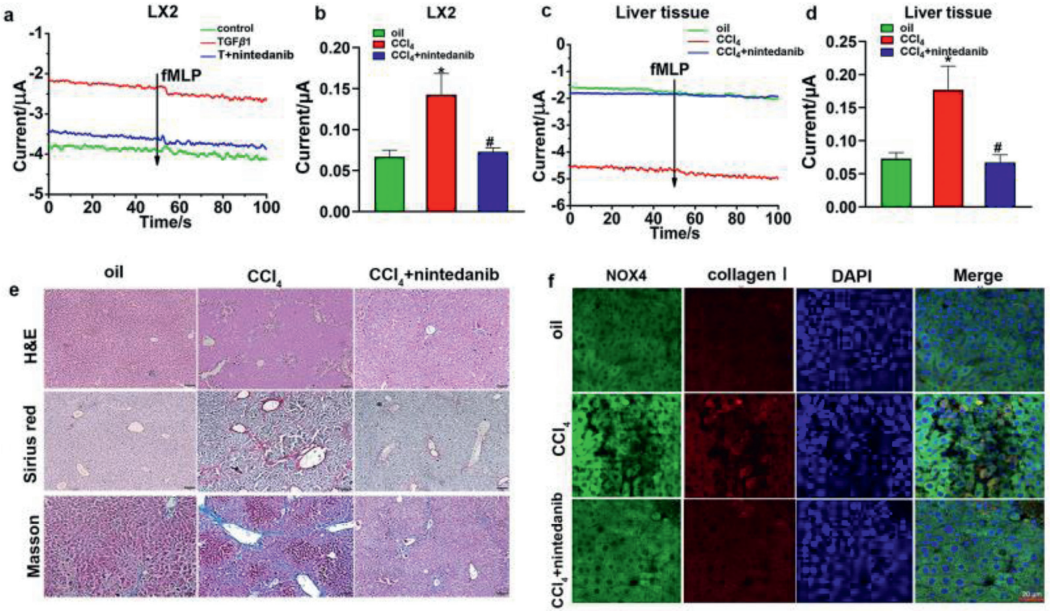

Fig. 4. (a, b) The levels of H_2O_2 in LX2 cells were detected by the sensor. (c, d) The levels of H_2O_2 in the liver tissues of mice were detected. The data are presented as the means ± SD, $n = 3$. $^{*}P < 0.05$ *vs.* oil. $^{\#}P < 0.05$ *vs.* CCl_4. H&E staining of liver tissues from the oil, CCl_4, and CCl_4 + nintedanib (30 mg/kg) groups. (e) Masson staining and Sirius red staining. Scale bar: 100 μm. (f) Immunofluorescence imaging of collagen I and NOX4 in liver tissues. Scale bar: 20 μm.

sor's response to changes in H_2O_2 in fibrotic liver tissue. Consistent with previously reported results [32], nintedanib improved carbon tetrachloride (CCl_4)-induced structural damage, inflammatory infiltration and collagen deposition in the liver (Fig. 4e). Our sensor not only detected changes in H_2O_2 in activated LX2 cells *in vitro* (Figs. 4a and b) but also sensitively detected changes in fibrotic liver tissue (Figs. 4c and d). The commercially available H_2O_2 detection kit was also used (Fig. S2c in Supporting information). Immunofluorescence analysis also showed that the NOX4 protein was highly expressed in CCl_4-induced hepatic fibrosis tissue and was enriched near the lesions of collagen deposition in comparison with that in the oil group (Fig. 4f). These results indicate that our sensor can be used as a means of evaluating drugs for the treatment of liver fibrosis.

In summary, we used a nonenzymatic electrochemical H_2O_2 sensor to detect H_2O_2 changes in fibrotic cells and tissues. PtNi-N-rGO can fully adsorb and catalyze H_2O_2 due to its small size PtNi nanoparticles and nitrogen doping rGO. The concentration of H_2O_2 is measured by the amperometric *i-t* curve technique by applying the reduction potential (relative to saturated calomel electrode (SCE), −0.6 V) and recording the current, thus achieving successful detection of H_2O_2 [27]. We summarized and analyzed H_2O_2 electro-reduction mechanism for nano-enzymatic based H_2O_2 sensor [26,27]. Detailed catalytic mechanism equation can be found in Supporting information. In this study, H_2O_2 was used as a molecular biomarker, and our sensor successfully captured H_2O_2 produced by TGFβ1-activated fibroblasts, expanding the application fields of electrochemical sensor [33]. In addition, the sensor could rapidly and sensitively detect H_2O_2 released in the lung and liver tissues of mice with fibrosis. Therefore, the H_2O_2 sensor can reflect the effects of drugs on fibrosis, and this technology can be used as a convenient means for fibrosis drug screening.

Declaration of competing interest

The authors declare that they have no known competing financial interests or personal relationships that could have appeared to influence the work reported in this paper.

Acknowledgments

This work was supported by the National Natural Science Foundation of Sichuan Province (Nos. 2022NSFSC1465, 2023NSFSC0525), Post-Doctor Research Project, West China Hospital, Sichuan University (No. 2021HXBH086), the Sichuan University postdoctoral interdisciplinary Innovation Fund (No. 10822041A2118) and Full-Time Postdoctoral Research Fund of Sichuan University (No. 20826041F4134).

Supplementary materials

Supplementary material associated with this article can be found, in the online version, at doi:10.1016/j.cclet.2023.108574.

References

[1] N.C. Henderson, F. Rieder, T.A. Wynn, Nature 587 (2020) 555–566.
[2] T.A. Wynn, J. Clin. Invest. 117 (2007) 524–529.
[3] A.L. Mora, M. Rojas, A. Pardo, et al., Nat. Rev. Drug Discov. 16 (2017) 755–772.
[4] S.B. Strock, J.K. Alder, D.J. Kass, J. Pathol. 244 (2018) 383–385.
[5] A.U. Wells, Lancet Respir. Med. 6 (2018) 735–737.
[6] L. Richeldi, H.R. Collard, M.G. Jones, Lancet 389 (2017) 1941–1952.
[7] W. Merkt, M. Bueno, A.L. Mora, D. Lagares, Semin. Cell Dev. Biol. 101 (2020) 104–110.
[8] M. Parola, M. Pinzani, Mol. Aspects Med. 65 (2019) 37–55.
[9] T. Zhang, X. He, L. Caldwell, et al., Sci. Transl. Med. 14 (2022) eaaz4028.
[10] M. Jain, E.A. Monclus, S. Rivera, et al., J. Biol. Chem. 288 (2013) 770–777.
[11] S.Smith E.Otoupalova, G. Cheng, et al., Compr. Physiol. 10 (2020) 509–547.
[12] Z. Tan, H. Sun, T. Xue, et al., Front. Cell Dev. Biol. 9 (2021) 730176.
[13] T. Xue, L. Yue, G. Zhu, et al., Liver Int. 43 (2023) 718–732.
[14] L. Lin, H. Gong, R. Li, et al., Adv. Sci. 7 (2020) 1903138.
[15] J. Liu, Z. Wu, Y. Liu, et al., J. Nanobiotechnol. 20 (2022) 213.
[16] D. Chanda, E. Otoupalova, S.R. Smith, et al., Mol. Aspects Med. 65 (2019) 56–69.
[17] R.M. Liu, K.A. Gaston Pravia, Free Radic, Biol. Med. 48 (2010) 1–15.
[18] R. Samarakoon, J.M. Overstreet, P.J. Higgins, Cell. Signal. 25 (2013) 264–268.
[19] K. Tsubouchi, J. Araya, S. Minagawa, et al., Autophagy 13 (2017) 1420–1434.
[20] N. Amara, D. Goven, F. Prost, et al., Thorax 65 (2010) 733–738.
[21] Y.Y. Sanders, X. Lyv, Q.J. Zhou, et al., JCI Insight 5 (2020) e137127.
[22] Z. Cao, T. Ye, Y. Sun, et al., Sci. Transl. Med. 9 (2017) eaai8710.
[23] J. Du, J. Sun, N. Li, et al., Acta Pharmacol. Sin. 42 (2021) 1090–1100.
[24] C. Wang, Y. Wang, G. Wang, et al., Anal. Chim. Acta 1097 (2020) 230–237.
[25] Y. Tian, L. Du, P. Zhu, et al., Biosens. Bioelectron. 176 (2021) 112899.

[26] Y. Yu, M. Pan, J. Peng, et al., Chin. Chem. Lett. 33 (2022) 4133–4145.
[27] Y. Yu, J. Peng, M. Pan, et al., Small Methods 5 (2021) e2001212.
[28] H. Liu, X. Wu, C. Gan, et al., Cell Prolif. 54 (2021) e13081.
[29] L. Yue, T. Xue, X. Su, et al., Eur. J. Med. Chem. 242 (2022) 114685.
[30] P. Kolb, C. Upagupta, M. Vierhout, et al., Eur. Respir. J. 55 (2020) 1901105.
[31] R.H. Hübner, W. Gitter, N.E. El Mokhtari, et al., BioTechniques 44 (2008) 507–517.
[32] L. Wollin, D. Togbe, B. Ryffel, Biomed. Res. Int. 2020 (2020) 3867198.
[33] J. Xu, J. Ma, Y. Peng, et al., Chin. Chem. Lett. 34 (2023) 107527.